



Enhanced Photocatalytic Activity of Titanium Dioxide Supported on Hexagonal Mesoporous Silica at Lower Coverage

QING DAI^{1,2,*}, NONGYUE HE¹, KUIPING WENG², BAOPING LIN²,
ZUHONG LU¹ and CHUNWEI YUAN¹

¹National Laboratory of Molecular & Biomolecular Electronics, Southeast University, Nanjing 210096, P.R. China; ²Department of Chemistry and Chemical Engineering, Southeast University, Nanjing 210096, P.R. China

Abstract. The photocatalytic activities of titanium dioxide (TiO₂) supported on hexagonal mesoporous silica (HMS), zeolite Y (NaY) were investigated by using the photodegradation of 2,4,6-trichlorophenol (TCP) as test reactions. It was found that the photocatalytic activity of TiO₂ on HMS was much higher than that of TiO₂ powders, and that of TiO₂ on NaY. It was also found that TiO₂/HMS had maximal photocatalytic activity at a lower Ti content. The larger the pore size of HMS used as the support of TiO₂, the better the photocatalytic activity of TiO₂ for degrading of organic pollutant. These observations suggested that the supported structure was a main factor responsible for enhancement of the photocatalytic activity of TiO₂. Characterization of the samples by TEM, XRD, BET, and UV-vis diffuse reflectance spectra indicated that the structures of HMS and TiO₂ were confirmed and TiO₂ did not enter into the HMS framework and was formed as nanoparticles on all supports.

Key words: photocatalytic activity, titanium dioxide, hexagonal mesoporous silica, zeolite Y

1. Introduction

The photocatalytic degradation of organic pollutants has attracted a great deal of attention in recent years [1–6]. Most of the research groups have exploited the favorable electronic and mechanical characteristics of TiO₂. This “semiconductor” has a band gap corresponding to photon absorption for $\lambda > 380$ nm so that it can be pumped with inexpensive UV lamps. The oxidation potential of the photogenerated hole exceeds 3.0 V. The solid is mechanically and chemically robust and resists both thermal and photochemical degradation. But now, with the emergence of environmental problem, cleanup is an issue of the highest priority, many research efforts are focused on improving the capability of photocatalytic systems to destroy pollutants in both water and gaseous systems. For engineering applications, the

* Author for correspondence. Tel: +8625 3792245; Fax: +8625 7712719; E-mail: qdai@seu.edu.cn

main drawback is the small size of the powder particles prepared by the usual industrial synthesis. This has led to a number of attempts to anchor TiO_2 on supports including glass beads [7, 8], fibre glass [9, 10], silica [11], electrode [12], clay [13] and zeolite [14, 15]. So far, these efforts have not produced materials which met all requirements of photocatalytic activity [16–18]. Moreover, supported TiO_2 is commonly reported to be less photoactive than the corresponding TiO_2 alone [19, 20].

Attempts to find a suitable support for TiO_2 should take into account several factors. First, TiO_2 has a polar surface and is not, itself, a good adsorbent for nonpolar organic molecules. Preconcentration of substrates on the surface, where photons are adsorbed is a desirable feature for oxidation kinetics. Second, the supports may be able to enhance catalytic properties ranging from surface acidity to reactive intermediate stabilization. This report deals with the first step toward a suitable support by means of a systematic exploration of several factors. We compare here the photocatalytic activity of pure TiO_2 alone, synthesized by the procedure which is also used in the preparation of the supported materials, with that of TiO_2 supported on hexagonal mesoporous sieve (HMS) and zeolite (NaY). The test reactions are degradation of 2,4,6-trichlorophenol (TCP), which is a major pollutant produced by paper mills and also a good model of environmental research [21]. The various solids are characterized by power diffraction (XRD), BET and UV-vis Diffuse reflectance spectra. In the photocatalytic measurements, we see indications of dependence on the structure of the supported materials which may point to specific stabilization of intermediates, but most strikingly, indications that improved adsorption of nonpolar organic molecules is favorable, as expected. The photocatalytic activity of TiO_2 /HMS using a lower Ti content is superior to that of TiO_2 nanoparticles.

2. Experimental

2.1. CHEMICALS

TCP (>99%) was purchased from Aldrich. NaY(Si/AL = 2.49) was purchased from the Petrochemical Institute of Fushun, China. The TiO_2 sol was synthesized by the method called acid-catalyzed sol-gel formation [22]. The HMS was synthesized under hydrothermal conditions according to the modified procedures described by Gontier and Tuel [23]. Other chemicals were of reagent grade and used as received.

2.1.1. TiO_2

TiO_2 colloid solutions were prepared by hydrolysis of the tetraisopropoxide, $\text{Ti}(\text{O}-i\text{-Pr})_4$, as follows: 25 mL of $\text{Ti}(\text{O}-i\text{-Pr})_4$ was added to 4 mL of isopropanol, then the mixture was added to 150 mL of distilled deionized water containing 2 mL of 70% nitric acid, keeping stirring for 6 h at about 75 °C. Approximately 150 mL

of TiO₂ colloid solutions which is stable for several months at 4 °C were obtained after removing the organic layer. The size of the colloidal particles determined by transmission electron microscopy (TEM) is around 10 nm. The concentration of the TiO₂ colloid solutions is 17.32 mg/mL.

2.1.2. HMS

The HMS was synthesized according to the following methods: the first solution (A) was prepared from 22.5 mL tetraethyl orthosilicate and 38 mL alcohol, the second solution (B) contained 0.027 mol alkylamine (dodecyl-, octadecyl-), 64.8 mL water and 0.002 mol hydrochloric acid. Solution A was added slowly to solution B under vigorous stirring. Stirring was maintained for about 15 min, and the solution was kept at ambient temperature for various periods. Then, the white solid was collected by filtration, washed several times with acetone, alcohol and distilled water, and dried at room temperature. Organic molecules were removed by calcination of the as-synthesized solid in air at 540 °C for 6 h. XRD and BET confirmed the structure of HMS.

2.2. PREPARATION OF SUPPORTED TiO₂ CATALYSTS

The supported catalysts were prepared by mixing TiO₂ colloid solutions with the powder of supports (HMS, NaY), subsequently the dried solid was calcined at 450 °C for 12 h. In a typical preparation of a supported photocatalyst, 4.5 g of a support, saturated with 10 mL of water for half an hour, was mixed with 9.1 mL of TiO₂ colloid solutions for one-hour with stirring. The mixture was dried by evaporation at 50 °C for 6 ~ 8 h, followed by heating at 120 °C overnight and finally the solid was calcined at 450 °C for 12 h. Then, the supported TiO₂ catalyst of 2% Ti content was obtained. By this procedure, a series of samples were prepared with different content of TiO₂ on each support. UV-vis diffuse reflectance spectra were used to confirm whether titanium entered the HMS structural framework.

2.3. CHEMICAL ANALYSIS OF TITANIUM DIOXIDE

A sample of the catalyst (0.2 ~ 0.3 g) was treated with the mixture of strong acids (HCl: H₂SO₄ = 1 : 1 by volume) for more than 1 week with occasional heating. The resulting suspension was diluted with 4 mol/L HCl. The titanium(IV) complex formed by the dissolved titanium(IV) with an excess of NH₄SCN was then extracted into a hexane phase in 5 ~ 10 min and its absorbance at 424 nm was recorded [24]. The absorbance is linear with the concentration of the titanium complex as confirmed by a calibration curve. The molar absorptivity was 31.620 at 424 nm. The measured contents of TiO₂ in each sample was close to the amount of titanium used during the preparation. In this report, the Ti content is reported as Ti% by weight.

2.4. CHARACTERIZATION OF THE SAMPLES

Powder X-ray diffraction patterns were recorded by Cu K α radiation ($\lambda = 1.554059 \text{ \AA}$) on a Rigaku D/max- γ A diffractometer. Surface areas were measured by four points BET method on a ASAP 2000 system, with nitrogen as the adsorption gas, at liquid nitrogen temperature. The pore sizes of HMS-type samples were determined by low-temperature nitrogen sorption on a Micromeritics ASAP-2000 Instrument Sorption Analyzer with BJH model, after the samples were degassed at 350 °C at 10^{-4} mmHg. The results were calculated by BET analysis using a program available with the instrument. High Resolution Electron Microscopy (HRTEM) was recorded using a JEOL 200cx instrument. The Diffuse UV-vis Reflectance Spectra of TiO₂ supported on the HMS were recorded, which reveal whether the Ti enters into the framework of the supported catalysts.

3. Photocatalytic Experiments

The photocatalytic activities of various catalysts were evaluated by measuring the loss of TCP. Prior to commencing illumination, a suspension containing 1.2 g of TiO₂/HMS catalyst and 50 mL of about 1.33 mM TCP was stirred continuously for 1 h. The concentration of substrate in the bulk solution at this point was used as the initial value for the further treatment and the solution concentration decreases in a definite time were used for calculating the extent of substrate adsorption on a catalyst. The reactions were carried out in a stirred glass flask by irradiation with UV light from a 300 W high-pressure mercury lamp enclosed in a quartz glass and cooled by water circulation to 25 °C during the experiments. In comparative runs, a total irradiation time was 140 min for each sample. At each interval of 20 min, a 2 mL sample solution was withdrawn by syringe from the irradiated suspension, and filtered through a Millipore filter membrane (0.45 pore size). The standard methods, either GC-MS or HPLC analyzed the filtrate. For contrast, the reaction was worked under the same conditions but using TiO₂ nanoparticles and TiO₂/NaY.

4. Results and Discussion

4.1. STRUCTURAL PROPERTIES AND COMPOSITION OF THE SAMPLES

4.1.1. TiO₂

Titanium dioxide can be prepared in three crystal forms: anatase, rutile, and brookite. Several reports suggested that TiO₂ in the anatase form had the highest photocatalytic activity. The morphology and structure of TiO₂ prepared in this study are shown in Figures 1 and 2, which indicate that the size of the colloidal particles is about 10 nm. The electron diffraction of the sample is also shown in Figure 2. According to this figure, the *D*-spacing can be calculated in the following equation:

$$D = \lambda \cdot \lambda / R, \quad \lambda = h / mv = 12.256 [V(1 + 9.788 \times 10^{-7} V)]^{-1/2},$$

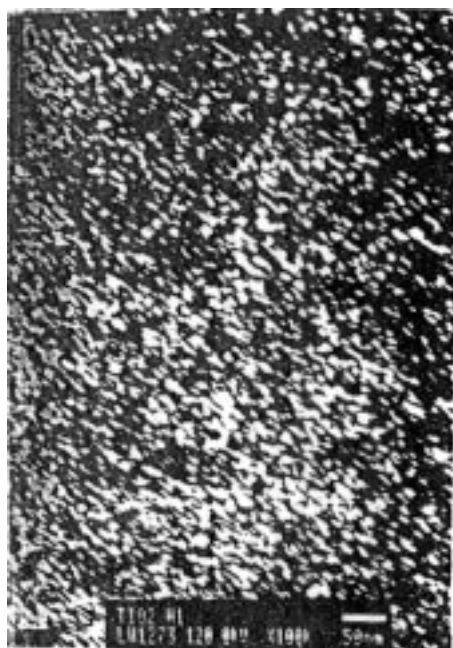


Figure 1. TEM morphology of TiO₂ colloidal particles.

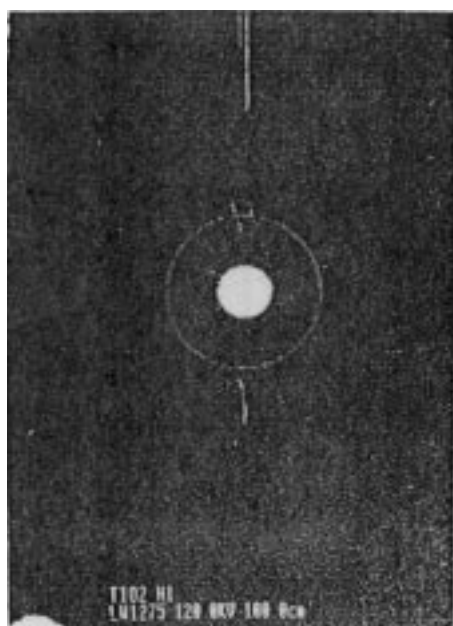


Figure 2. Electron diffraction pattern of TiO₂ colloidal particles.

Table I. Electron diffraction pattern data for TiO₂ nanoparticles

R	$D_{\text{anatase}}^{\text{theory}}$ [5]	$D_{\text{experiment}}$
0.96	3.52	3.49
1.44	2.38	2.34
1.82	1.89	

Table II. Structural properties of HMS and zeolite

Sample	a_0 (Å)	S_{BET} (m ² /g)	V (cm ³ /g)	f_P (nm)	Wall thickness (ns)
HMS(12)	48.5	1064	0.62	2.5	2.4
HMS(18)	61.2	1021	0.74	3.4	2.7
NaY	24.7		0.31	0.7	

* $a_0 - f_P = \text{wall thickness}$.

where L is the distance between the test sample and the film, V is the accelerating voltage, R is the radius of the diffraction ring, λ is the wavelength of electron wave. The calculation results are shown in Table I, which indicates that the anatase is the main constituent of TiO₂ colloid solution prepared by ourselves.

4.1.2. HMS

We mainly selected dodecylamine (DDA) and octadecylamine ODA as two different templates to synthesize the pure hexagonal mesoporous silica. The X-ray diffraction patterns of the template free samples are shown in Figure 3. It is evident that the template with longer chain length engenders the product showing only one strong peak in the lower angle region. The absence of high Bragg reflections in HMS materials was attributed to the small scattering domain size effect. After calcination, moreover, the diffraction peak shifted right and the intensities of peaks were increased. This suggested that the process of calcination increased the overlapping of the inorganic species, shrunk the framework of HMS and improved the order of the pore accumulation. The chemical composition, unit cell parameter, surface areas of chemical composition, surface areas, pore sizes and wall thickness after calcination are reported in Table II. From Table II, we can also find that all samples exhibit nanometer pore sizes around 3 nm and large surface area. The HRTEM pictures of the hexagonal structure of the four template free samples display hexagonal ordered pores, whose size is the same as that determined by N₂ adsorption at low temperature (Figures 5 and 6).

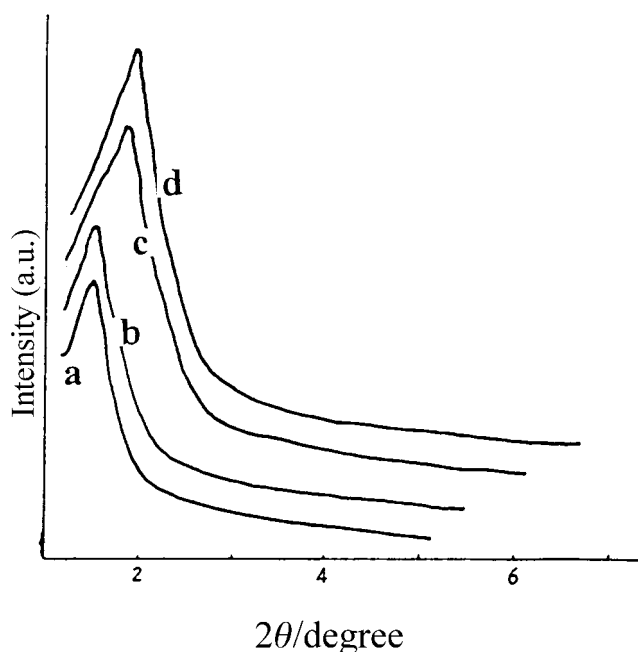


Figure 3. XRD patterns of HMS synthesized by different templates. (a) A *S*-synthesized sample (ODA). (b) A *S*-synthesized sample (DDA). (c) Calcined sample (ODA). (d) Calcined sample (DDA).

4.1.3. TiO₂/HMS

As will be seen below, the TiO₂ supported on the HMS yielded the most interesting photochemistry. To show the influence of the Ti content on the physicochemical properties of the TiO₂/HMS, we have prepared samples with Ti content of 2%, 4%, 8%, 16% and 32%. All these catalysts with different Ti content were examined using diffuse UV-vis spectra with a photospectrometer, which is equipped with a Praying Mantis (light collector) (see Figure 4). This technique has been used extensively for the characterization of the nature and coordination of Ti⁴⁺ ions in zeolites. From Figure 4, no peak was observed around 220 nm, indicating the absence of Ti in the framework of the HMS.

4.2. PHOTOCATALYTIC ACTIVITY

The hypothesis on which the study was initiated is that the photocatalysis occurs on the TiO₂ catalyst surface so that the adsorption properties of the catalyst will be a significant factor including crystal form of TiO₂ and property of support. We have used one substrate, TCP, in the presence of HMS and zeolite NaY supports when samples were illuminated at a wavelength longer than the lowest band in the

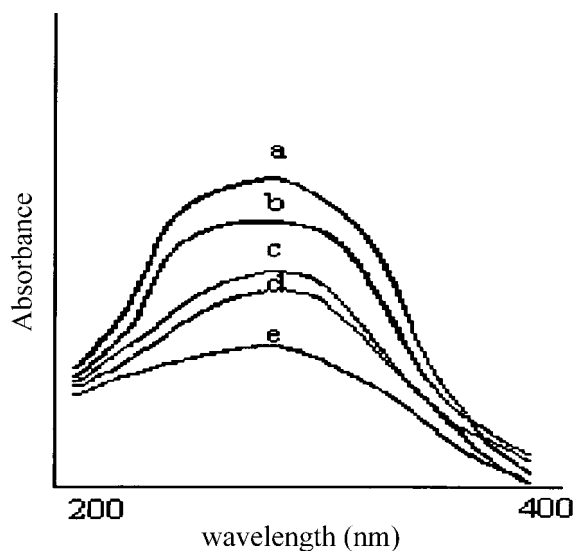


Figure 4. Diffuse reflectance of UV-vis spectrum of TiO_2 species in HMS. (a) 4% Ti/HMS (18), (b) 4% Ti/HMS (12), (c) 8% Ti/HMS (12), (d) 16% Ti/HMS (12), (e) 32% Ti/HMS (12).



Figure 5. TEM of HMS templated by dodecylamine.

substrate spectrum ($\lambda > 380$ nm). The supports used in this work had no observable photocatalytic activities. In all reactions, the photodegradation kinetics using TiO_2 as photocatalysts were satisfactorily fitted in with the first-order rate law. The present study showed similar results.

We began with a review of the behavior of the pure TiO_2 prepared by the present procedure when the Ti loading in the supports increased. The rate constant, K ,

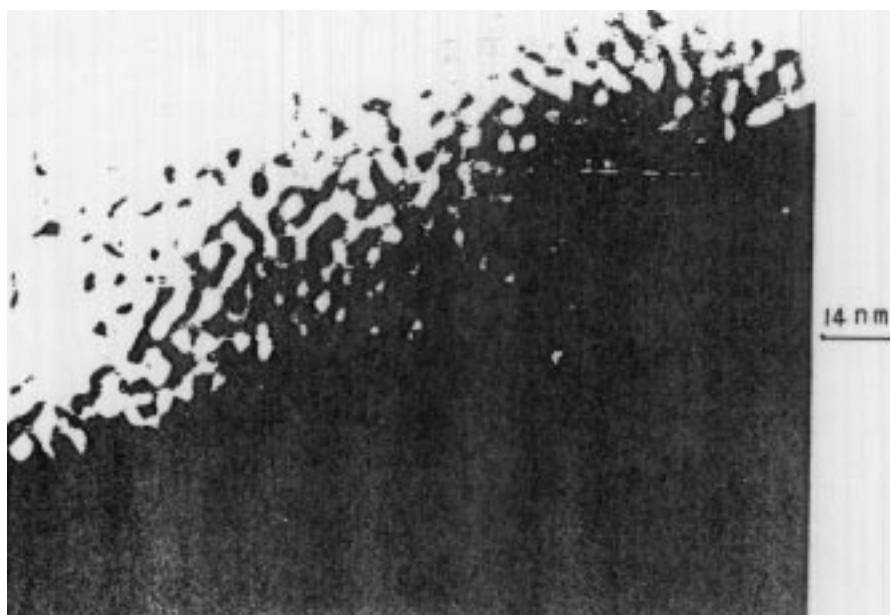


Figure 6. TEM of HMS templated by dodecylamine.

increased with the enhancement of TiO₂ concentration, but was invariable when above about 1 g/L, which has been frequently observed in photocatalysis, and is interpreted to indicate that with sufficient loading all light is absorbed by TiO₂ and the further addition of catalyst cannot accelerate the reaction. Thus we selected the concentration of 0.8 g TiO₂/L or corresponding to this concentration, which was used in all the reaction system.

Next, we considered the behavior of this TiO₂ supported on HMS and NaY. In the dark, prior to illumination, the TCP concentration in solution decreases very little in the presence of the appropriate concentration of HMS-supported catalyst. The dark adsorption of TCP on the NaY-supported catalyst sample and TiO₂ was not detectable under blank control conditions. Table III showed that the data collected from HPLC related to the photodegradation of TCP with TiO₂ supported on HMS and related materials, which indicates the HMS supported catalyst was the most efficient in the degradation of TCP among the three kinds of catalysts (TiO₂, TiO₂/HMS and TiO₂/HMS). It is attractive to suggest that this is the consequence of the relative adsorption behavior of the catalysts, especially the structure of the supports. Besides that HMS produces the most efficient support of the catalyst, we can also see that when HMS(12) is changed into HMS(18), e.g., the pore sizes of the hexagonal molecular sieves increased (Figure 2), and the photocatalytic activity is further enhanced (No. 4 and No. 8 in Table III). On the HMS(18) sample, dark adsorption was similar to the HMS(12). This clearly suggests that the enhanced photoactivity compared with HMS(12) may have something to do with the mesoporous structure.

Table III. Data collected from HPLC related to the photodegradation of TCP with TiO₂ supported on HMS and related materials

Catalysts	Ti content (wt%)	Conversion (%)						
		20 min	40 min	60 min	80 min	100 min	120 min	140 min
TiO ₂	60	6.1	9.9	15.3	22.4	30.7	35.2	40.8
TiO ₂ /NaY	4	6.0	8.7	16.3	21.1	29.8	34.5	37.8
TiO ₂ /HMS(12) ^a	2	6.5	11.2	16.9	25.3	34.8	44.7	56.1
TiO ₂ /HMS(12) ^a	4	6.7	12.3	18.1	27.8	38.9	47.7	61.3
TiO ₂ /HMS(12) ^a	8	12.8	23.4	31.9	42.1	53.4	65.9	84.2
TiO ₂ /HMS(12) ^a	16	29.2	44.6	69.7	97.2			
TiO ₂ /HMS(12) ^a	32	37.3	55.1	71.2	99.6			
TiO ₂ /HMS(18) ^a	4	6.8	20.4	35.7	51.6	64.9	75.2	90.9

^a The numbers in parentheses are the carbon numbers in the chain of the primary amines as template.

We have seen that in addition to the adsorption factor the HMS structure may also be a factor associated with the photocatalytic activity of TiO₂/HMS. With the geometric series increase of Ti content in TiO₂/HMS(12) support catalysts, the photocatalytic activities did not increase with the geometric series increase. However, when the TiO₂/HMS(12) with lower TiO₂ content coverage is around 16% (Ti content in TiO₂/HMS(12)), the photocatalytic activities were almost optimal. This suggests that a higher Ti content in TiO₂/HMS(12) is not necessary.

The intermediates detected by GC-MS during the course of the degradation were chloromaleic acid, chlorofumaric acid, maleic acid and fumaric acid. Following the photolysis, the absorption bands corresponding to TCP in the UV spectra disappeared completely, which indicated complete disappearance of TCP. The observation of increased absorbance in the 265–295 nm region at short illumination time was attributed to the formation of reaction intermediates. These observations were similar to those observed in the TiO₂ reaction, but the catalytic activity of TiO₂ supported on HMS was much higher than that of TiO₂ nanoparticles. However, when NaY was employed as a support of TiO₂, it was less photoactive than the corresponding TiO₂ alone. The substrate conversions were also monitored by HPLC (ultraviolet detection at 248 nm, and experimental data are summarized in Table III). This showed that the larger the pore size of HMS, the better the photocatalytic activity for the degradation of TCP. The high efficiency at low loading may be the most significant result of this exploratory study.

Acknowledgements

This work is supported by the Key Laboratory of Photochemistry of Chinese Academy of Science and Chinese Postdoctoral Science Foundation.

References

1. A. L. Linsebigler: *Chem. Rev.* **95**, 735 (1995).
2. M. R. Hoffmann and S. T. Martin: *Chem. Rev.* **95**, 69 (1995).
3. M. A. Fox and M. T. Dulay: *Chem. Rev.* **93**, 341 (1993).
4. M. Halmann: in J. F. Rabet (ed.), *Photocatalyzed Oxidation in Aqueous Solutions*, Chap. 3. CRC Press, Inc., U.S.A. (1992), pp. 75–102.
5. U. Stafford, K. A. Gray, and P. V. Kamat: *HCR Advanced Education Review*, **3**, 77 (1996).
6. P. V. Kamat: *Chemtech.* **6**, 22 (1997).
7. R. W. Mattews: *J. Phys. Chem.* **102**, 6853 (1998).
8. M. A. Anderson, H. Kikkawa, M. Edwards et al.: *J. Catal.* **127**, 167. (1991).
9. K. Hofstandler, R. Bauer, S. Novalic et al: *Environ. Sci. Technol.* **28**, 670 (1994).
10. R. W. Matterws: *J. Phys. Chem.* **91**, 405 (1987).
11. S. Sato: *Langmuir* **14**, 1156 (1998).
12. K. Vinodgopal, S. Hotchandari, and P. V. Kamat: *J. Phys. Chem.* **97**, 9040 (1993).
13. H. Yoneyama, S. Haga, and S. Yamanaka: *J. Phys. Chem.* **93**, 4833 (1989).
14. K. J. Green: *J. Chem. Soc. Faraday Trans.* **89**, 1816 (1993).
15. X. Liu, K. Iu, and J. K. Thomas: *J. Chem. Soc., Faraday Trans.* **89**, 1816 (1993).
16. M. A. Fox, K. E. Doan, and M. T. Dulay: *Res. Chem. Intermed.* **20**, 711 (1994).
17. X. Liu, K. K. Iu, and J. K. Thomas: *J. Chem. Soc. Faraday Trans.* **89**, 1867 (1993).
18. O. Legrini, E. Oliveros, and A. M. Braun: *Chem. Rev.* **93**, 671 (1993).
19. R. W. Mattews: *Wat. Res.* **24**, 653 (1990).
20. J. Sabate, M. A. Anderson, and M. A. Aguado: *J. Mol. Catal.* **71**, 57 (1992).
21. Ning-Ping Huang: *J. Photochemistry and Photobiology A: Chemistry* **108**, 229 (1997).
22. A. Sorokin et al.: *Sciences* **268**, 1163 (1995).
23. S. Gontier and A. Tuel: *Zeolites* **15**, 1 (1995).
24. J. Wang and P. C. White: *Anal. Chem.* **3**, 31 (1959).
25. J. Klaas, G. Schulz-Ekloff, and N. I. Jaeger: *J. Phys. Chem.* **101**, 1307 (1997).

